FACTA UNIVERSITATIS
Series: **Mechanical Engineering** Vol. 21, Nº 1, 2023, pp. 137 - 150
https://doi.org/10.22190/FUME221215005H

Original scientific paper

FRACTAL DIMENSIONS OF A POROUS CONCRETE AND ITS EFFECT ON THE CONCRETE'S STRENGTH

Chun-Hui He[1], Chao Liu[1,2]

[1]School of Civil Engineering, Xi'an University of Architecture and Technology, Xi'an, China
[2]School of Science, Xi'an University of Architecture and Technology, Xi'an, China

Abstract. *All mechanical properties of a porous medium depend upon its fractal dimensions, however, how to measure the fractal dimensions is still an open issue. This paper adopts the two-scale fractal theory to calculate fast and effectively the fractal dimensions of a porous concrete. Of the concrete's properties that have been fascinating engineers and scientists, by far the most perplexing is the effects of its porosity and pore size on concrete's strength. Though there were many ad hoc empirical formulae for predicting the strength, much deviation arose for practical applications. Here a dimensionless model and the fractal theory are adopted to insight theoretically into the effects, and for the first time ever, some physically relative and mathematically reliable formulations are proposed. Additionally nano/micro particles' size and distribution can also be used for theoretical prediction of the concrete's strength, it shows that the boundary-induced force occurs when the particles tend to micro/nanoscales. The present theory sheds new light on the optimal design of various functional concretes.*

Key words: *Two-scale fractal, Geometric potential, Dimensionless analysis, Hall-Petch effect, Porosity*

1. INTRODUCTION

A porous medium always behaves extremely attractively compared to its continuum partner, the latter is focus of the continuum mechanics, which has matured into a fully-fledged theory, and has laid the foundation for the mechanical engineering, however, there is no universal theory for porous problems. Xue and Liu [1] found that a porous medium with a hierarchical structure has an excellent heat insulation. Xo, et al. [2] revealed the mechanism of heat prevention for cocoon-like hierarchy. Xue, et al. [3] further elucidated cocoon's biomechanism using the fractal theory. Hierarchical porous materials are now

Received: December 15, 2022 / Accepted February 01, 2023
Corresponding author: Chao Liu
School of Civil Engineering, Xi'an University of Architecture and Technology, Xi'an, China
E-mail: chaoliu@xauat.edu.cn

widely used for high-rate electrochemical capacitive energy storage [4], supercapacitors [5] and energy harvesting [6,7]. Nano/micro scale porous membranes have extremely high permeability and extremely small pressure drop [8-11], the diffusion process in a porous medium (e.g. water) has attracted much attention in the academic community, because the seemingly stochastic diffusion process is actually deterministic in a fractal space, making the impossible possible [12,13,14]. The vibrating process in air can also be considered in a fractal space, and a new discipline, the fractal vibration theory, has been skyrocketing [15,16,17]. The fractal theory and the artificial intelligent have been successfully applied to investigate the hardness properties of tool steel alloys [18,19,20].

Some phenomena arising in porous media cannot be explained by continuum mechanics, where the smooth space is the footstone. This paper focuses on the most commonly used porous material on the Earth, that is the concrete [21,22,23], using the fractal theory [24].

2. Fractal Dimensions

All mechanical properties of a continuum medium are relative to its dimensions, for example, its volume scales with the cube of the measured size

$$V \propto r^3 \tag{1}$$

where V is the volume, r is the measured size. Similarly for a porous medium, its volume can be written as

$$V \propto r^\alpha \tag{2}$$

where α is the fractal dimensions. In a fractal space with a fractal dimensionality α, the volume is a measurement of the measured size. The relation of the fractal dimensionality α and the volume can be expressed in Eq. (2). When α=3, it becomes a continuum, and when α=0, it is an empty pore.

Zuo and Liu elucidated that the mechanical and electrical properties of a composite depend upon the fractal dimensions [25], Mandelbrot, et al. revealed that fracture property of metals can be effectively explained by the fractal dimensions [26]. Babič, et al. elucidated that the fractal dimensions are relative to the material's surface characteristics and mechanical property [18,19,20]. However how to calculate the value of the fractal dimensions is a difficult problem, and mathematicians and engineers will be captivated by an effective and reliable measurement.

There are many methods to calculate fractal dimensions, among which the Hausdorff dimensions are the most used one, its definition is [24, 26]

$$\alpha = \frac{\ln N}{\ln r} \tag{3}$$

where N is new measured units when we measure the fractal pattern using a reduced $1/r$ scale. Taking the Cantor set as an example, when we use a reduced 1/3 scale, we find two new units, N=2, so α=ln2/ln3.

But for a porous medium, we might know only its porosity, then how to calculate its fractal dimensions? We consider a Sierpiński-like porous area as shown in Fig. 1. When the porosity is zero, the area is two dimensional; while when the porosity equals to one, the area is zero dimensional, so it is obvious that $0<\alpha<2$. The Sierpinski carpet is a pure mathematical concept, the first cascade is similar to Fig. 1, however, each unit can continue iteration to form a Hausdorff dimensions of α=ln8/ln3 when C=L/3.

Feng, et al. [27] suggested the following formulation to calculate its fractal dimensions

$$\alpha = \frac{\ln(L^2 - C^2)}{\ln L} \tag{4}$$

where L^2 and C^2 are the areas of the measured unit and the porosity, respectively.

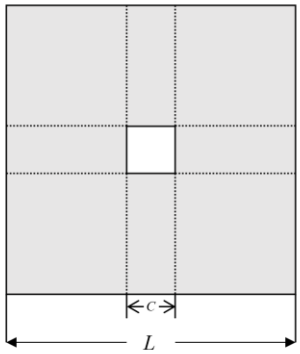

Fig. 1 A Sierpiński-like porous area

According to the definition of Eq. (4), we have

$$\lim_{C\to 0}\alpha = \lim_{C\to 0}\frac{\ln(L^2 - C^2)}{\ln L} = 2 \tag{5}$$

and

$$\lim_{C\to L}\alpha = \lim_{C\to L}\frac{\ln(L^2 - C^2)}{\ln L} \to -\infty \tag{6}$$

Though Eq. (5) meets the continuum assumption for a continuous medium, Eq. (6) is not physically inconsistent. Kong [28] suggested the following modified one

$$\alpha = \frac{\ln(L^2 / C^2 - 1)}{\ln(L / C)} \tag{7}$$

It is interesting to note that most natural materials have fractal dimensions closed to 1.618, the golden mean [29,30]. The fractal dimensions are also the key factor affecting a porous concrete's properties, Rieu and Sposito suggested the following formulation [31]:

$$\varphi = 1 - \left(\frac{r_{\min}}{r_{\max}}\right)^{3-\alpha_{\text{pore}}} \tag{8}$$

where φ is the porosity, $r_{\min}$ and $r_{\max}$ are the largest and smallest pore radiuses, respectively, α_{pore} is the fractal dimensions of the pore space.

Yu [32] pointed out that Eq. (8) is physically inconsistent, because for a continuum medium, we have α_{pore} =0 and φ=0; on the other hand, for the full porosity, α_{pore} =3 and φ=1. For the both cases, Eq. (8) gives wrong results. Yu suggested that following one [32]:

$$\varphi = c\left(\frac{r_{\min}}{r_{\max}}\right)^{3-\alpha_{pore}} \tag{9}$$

For a porous concrete, c=1, and Eq. (9) becomes

$$\varphi = \left(\frac{r_{\min}}{r_{\max}}\right)^{3-\alpha_{pore}} \tag{10}$$

Eq. (10) is physically consistent and mathematically reliable. But in practical applications, we have difficulty in determining $r_{\min}$ and $r_{\max}$, and its fractal dimensions can not be calculated through the porosity.

In this paper we adopt the two-scale fractal dimensions [33-35], which uses two scales, L and C, to measure the area for Fig. 1. When we use the scale of L, any pores with sizes less than L are ignored, so the area is L^2 with a two-dimensional property; when we measure it using a scale of C, its area becomes L^2-C^2. According to the definition of the two-scale fractal dimensions [33-35], we have

$$\frac{2}{\alpha} = \frac{L^2}{L^2 - C^2} \tag{11}$$

or

$$\alpha = \frac{2(L^2 - C^2)}{L^2} \tag{12}$$

For a porous concrete, when using a large scale, we can obtain its volume, V, with a three-dimensional property; while if we use a micro scale, the porous structure can be found, and the two-scale fractal dimensions for the concrete can be calculated through the following relationship [33]:

$$\frac{V - V_{\text{pore}}}{V} = \frac{\alpha}{3} \tag{13}$$

where V_{pore} is the total volume for pores. The porosity can be expressed as

$$\varphi = \frac{V_{\text{pore}}}{V} \tag{14}$$

So the two-scale fractal dimensions of the porous concrete can be calculated as

$$\alpha = 3(1-\varphi) \tag{15}$$

The fractal dimensions for the porous space in the concrete can be expressed as

$$\alpha_{pore} = 3 - \alpha = 3\varphi \tag{16}$$

The two-scale theory has become an effective tool to various discontinuous problems [36-40].

3. CONCRETE'S STRENGTH VS. FRACTAL DIMENSIONS

Concrete is a porous material, and the porosity and the pore size significantly affect the concrete's properties, especially its strength. There are many empirical formulae to express the relationship between the strength and its pore structure. The most famous one is [41, 42, 43]

$$F = F_0 (1-\varphi)^m \tag{17}$$

where F is the concrete's strength, F_0 is the strength of its continuum partner with zero porosity, m is an empiric constant, φ is the porosity.

Eq. (17) reflects only the effect of porosity, and the pore size is not considered. Kumar and Bhattacharjee suggested the following one [43]

$$F = F_0 K \frac{(1-\varphi)}{r^{1/2}} \tag{18}$$

where K is a constant, r is the pores' average radius.

In Eq. (17), the physical understanding of the parameter m lacks, and there is no practical criterion for choosing its value. Though Eq. (18) considers the effects of porosity and pores' size, the parameter K also lacks its physical meaning. The main problem of Eq. (18) is that the parameter K is dimension-related and physically irrelative. We re-write Eq. (18) in the form

$$\frac{F}{F_0} = K \frac{(1-\varphi)}{r^{1/2}} \tag{19}$$

When the porosity φ tends to zero, we have r=0, the concrete becomes a continuum medium and Eq. (19) implies that F/F_0 becomes infinitely large instead of $F/F_0=1$, so this is physically irrelative. Furthermore the left side of Eq. (19) is dimensionless, so the dimension of K has to be $m^{1/2}$. The value of K is different if r uses different dimensions, e.g., nanometer or micrometer. In order to resolve this apparent contradiction, the dimensionless analysis [44,45] can be powerfully applied, which is the central dogma of complex problems. Using the dimensionless analysis, Estrada-Diaz, et al. [44] found a useful mathematical formulation for electrospinning, He, et al. [45] established a bond stress-slip model for 3-D printed concretes, and Kong [28] found a totally new friction law for porous fabrics. According to the dimensionless analysis, Eq. (15) can be modified as

$$\frac{F}{F_0} = K_{dimensionless} (1-\varphi)^a \left(\frac{r_0}{r_m}\right)^b \tag{20}$$

where $K_{dimensionless}$ is a material constant, a and b are constants to be determined later, r_m is the average radius, r_0 is the porosity size of a reference pore, it can be the minimal/maximal porosity size.

Eq. (20) is a dimensionless formula, so it is physically relative and mathematically reliable. In order to determine the value of a, we write down the concrete's strength in the form

$$F = \sigma A \tag{21}$$

where σ is the stress, A is the contacted section area. Considering the porosity, the whole volume can be calculated as

$$V = V_0 (1-\varphi) \tag{22}$$

where V_0 is the sample's total volume.

The section area scales approximately with

$$A \propto V^{2/3} \tag{23}$$

So we have

$$A = KV^{2/3} = K_{dimensionless} V_0^{2/3} (1-\varphi)^{2/3} \tag{24}$$

According to the above relationships, we obtain

$$F = K_{dimensionless} \sigma V_0^{2/3} (1-\varphi)^{2/3} = K_{dimensionless} F_0 (1-\varphi)^{2/3} \tag{25}$$

where F_0 is the strength with zero porosity.

If we have the section's area porosity, p, the actual area can be written as

$$A = A_0 (1-p) \tag{26}$$

where A_0 is the section area when p=0.

Eq. (21) becomes

$$F = \sigma A_0 (1-p) \tag{27}$$

According to Eq. (23), the area porosity and the volume porosity have the following approximate relationship

$$(1-p) \propto (1-\varphi)^{2/3} \tag{28}$$

After a simple calculation, we have

$$F = K_{dimensionless} \sigma A_0 (1-p) = K_{dimensionless} F_0 (1-\varphi)^{2/3} \tag{29}$$

which is the same as Eq. (25).

According to the above analysis, the value of m in Eq. (17) and a in Eq. (20) should be approximately 2/3. Eq. (17) should be corrected as

$$F = K_{dimensionless} F_0 (1-\varphi)^{2/3} \tag{30}$$

In Ref. [42], m=8.15, this large deviation is due to the ignorance of the effect of pores' size. When the pores' size tends to micro/nano scales, the size effect [46] becomes enormous. Now we correct Eq. (20) as

$$\frac{F}{F_0} = K_{dimensionless}(1-\varphi)^{2/3}(\frac{r_0}{r_m})^b \tag{31}$$

To understand the parameter b, we explain the size effect [46] through the geometric potential theory [47]. When the pores' size tends to nano/micro scales, high surface energy (geometric potential) [47] can be produced. The geometric potential theory assumes that any surface produces a boundary-induced force, and it can explain many complex phenomena, for examples, Fangzhu's absorption of water molecules from the air [48,49], the nanofiber's wetting [47], and the cell orientation [50].

In order to use the geometric potential theory [47], we modify Eq. (31) in the form

$$\frac{F}{F_0} = K_{particle}(1-\varphi)^{2/3}(\frac{R_0}{R_m})^b \tag{32}$$

where $K_{particle}$ is a geometrical parameter, R_m is the average radius of the particles in the concrete, R_0 is the reference size. The geometric potential of particles can produce a surface force [47]:

$$f = -\frac{d\Pi}{dR_m} \tag{33}$$

where Π is the geometric potential produced by the particles. Generally, it can be expressed as [47]

$$\Pi \propto \frac{1}{(R_m)^\beta} \tag{34}$$

where β is the geometrical parameter. For a sphere like the Sun, β=1, which leads to Newton's gravity.

The concrete's strength due to nano/micro particles can be expressed as

$$F \propto \frac{K_{particle}}{(R_m)^b} \tag{35}$$

where $b=\beta+1$. Generally b=1/2 for the qualitative analysis as that in Hall-Petch effect [51].

$$\frac{F}{F_0} = K_{particle}(1-\varphi)^{2/3}(\frac{R_0}{R_m})^{1/2} \tag{36}$$

Generally we have R_m scales with r_m, so Eq. (36) can be expressed as Model I:

$$\frac{F}{F_0} = K_{dimensionless}(1-\varphi)^{2/3}(\frac{r_0}{r_m})^{1/2} \tag{37}$$

Using the experimental data given in Ref. [43], $K_{\text{dimensionless}}$ and r_0 in Eq. (37) can be identified, and finally for the studied concrete of Ref. [43], we have

$$\frac{F}{F_0} = 52.9(1-\varphi)^{2/3}\left(\frac{13.64}{r_m}\right)^{1/2} \tag{38}$$

Fig. 2 shows the comparison between the theoretical prediction of Eq. (38) and experimental data given in Ref. [43], and a relative agreement is seen. The deviation arises in various factors, the main factor is the pore size distribution because, in our theory analysis, only average pore size is considered.

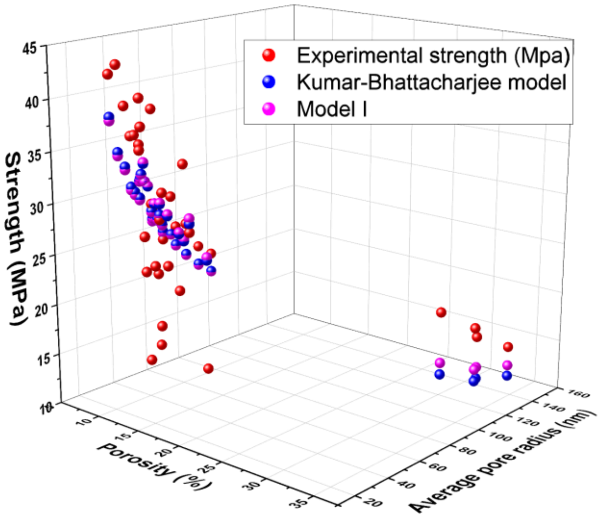

Fig. 2 Comparison between the theoretical prediction of Eq. (38) and experimental data given in Ref. [43]

As discussed above, b=1/2 is only used for the qualitative analysis. To understand the parameter b, the fractal theory has to be adopted.

As the concrete's strength is reflected by the contacted area, in a fractal space, the area and the volume have the following scaling relationship:

$$A \propto V^{(\alpha-1)/\alpha} \tag{39}$$

When α=3, we have the well-known 2/3 scaling law:

$$A \propto V^{2/3} \tag{40}$$

For a 4-dimensional space, we have

$$A \propto V^{3/4} \tag{41}$$

This 3/4 scaling law plays an important role in life science [52].

In a fractal space, Eq. (39) holds exactly, and Eq. (23) is approximate one, so Eq. (37) can be further improved as Model II:

$$\frac{F}{F_0} = K_\alpha (1-\varphi)^{(\alpha-1)/\alpha} (\frac{r_0}{r_m})^{1/2} \tag{42}$$

where K_α is a geometric parameter, α=3(1-φ).

Using the experimental data given in Ref. [43] to determine K_α and r_0 in Eq. (42), we have

$$\frac{F}{F_0} = 44.0(1-\varphi)^{(\alpha-1)/\alpha} (\frac{19.47}{r_m})^{1/2} \tag{43}$$

Fig. 3 shows the comparison between the theoretical prediction of Eq. (43) and experimental data given in Ref. [43].

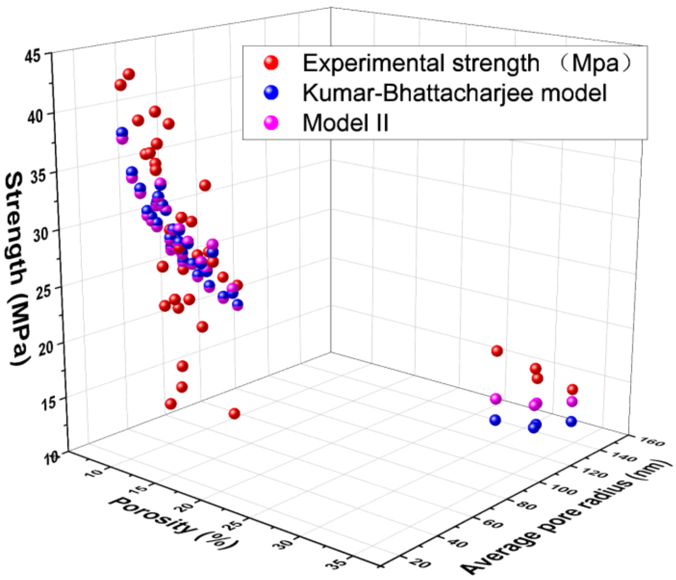

Fig. 3 Comparison between the theoretical prediction of Eq. (43) and experimental data given in Ref. [43].

We write the concrete's strength in the form

$$F = K_{particle}\sigma V^c (\frac{1}{R_m})^d = K_{particle} F_0 V_0^{c-2/3} (1-\varphi)^c (\frac{1}{R_m})^d \tag{44}$$

where K_{particle} is a geometrical constant, c and d are constants. According to the dimensionless analysis, the following equation should be satisfied:

$$3(c-\frac{2}{3}) - d = 0 \tag{45}$$

So we have Model III:

$$\frac{F}{F_0} = K_{particle} V_0^{c-2/3} (1-\varphi)^c (\frac{1}{R_m})^{(3c-2)}, c > 2/3 \tag{46}$$

and

$$\frac{F}{F_0} = K_{pore} V_0^{c-2/3} (1-\varphi)^c (\frac{1}{R_m})^{(3c-2)}, c > 2/3 \tag{47}$$

Eq. (46) or Eq. (47) reveals that the concrete's strength depends also upon its volume. Using the experimental data given in Ref. [43], we have approximately the following formulation:

$$\frac{F}{F_0} = 136.2(1-\varphi)^{0.798} (\frac{1}{r_m})^{0.394} \tag{48}$$

Fig. 4 shows the comparison between the theoretical prediction of Eq. (48) and experimental data given in Ref. [43].

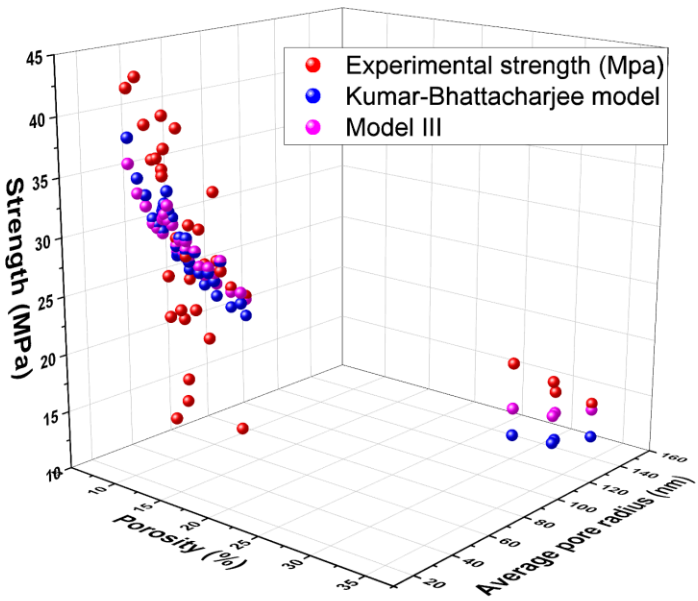

Fig. 4 Comparison between the theoretical prediction of Eq. (47) and experimental data given in Ref. [43].

Table 1 Comparison of our two models with experimental data [43]

Porosity (%)	Average pore radius (nm)	Strength (MPa)	K-B model[43] (MPa)	Model I (MPa)	Model II (MPa)	Model III (MPa)
12.96	34.3	18.3	30.3	30.4	30.4	30.1
11.93	38.7	28.4	28.9	28.9	28.8	29.0
10.87	58.7	26.8	23.7	23.6	23.6	24.8
11.1	41.3	22.7	28.2	28.1	28.1	28.4
13.53	42.3	21.5	27.1	27.3	27.3	27.6
12.75	26.6	27.5	34.5	34.6	34.6	33.4
10.8	39.3	29.7	29.0	28.9	28.8	29.1
10.83	52.9	26.8	25.0	24.9	24.8	25.9
11.8	45.8	30.3	26.6	26.6	26.5	27.1
11.22	31.2	35.3	32.4	32.3	32.3	31.7
11.5	30.4	40.3	32.7	32.7	32.6	32.0
9.26	28.1	43.2	34.9	34.6	34.4	33.7
10.38	41.9	38.7	28.2	28.1	28.0	28.5
16.55	34.2	28.3	29.1	29.6	29.8	29.1
9.5	23	42.5	38.5	38.1	38.0	36.4
9.63	30.3	39.3	33.5	33.2	33.1	32.6
33.7	146.9	14.2	11.2	12.3	13.1	13.6
33.14	126.7	16.4	12.1	13.3	14.1	14.5
11.22	41.6	15.5	28.1	28.0	27.9	28.3
12.04	35.4	24	30.2	30.2	30.1	30.0
11.39	71.3	23.2	21.4	21.4	21.3	22.9
12.23	31.2	14.9	32.1	32.1	32.1	31.5
15.37	49.6	13.6	24.5	24.8	24.9	25.4
12.01	30.5	23.7	32.5	32.5	32.5	31.8
10.38	47.5	25.7	26.5	26.4	26.3	27.1
10.4	68.3	23.9	22.1	22.0	21.9	23.5
11.3	43	30.7	27.6	27.5	27.5	27.9
13.55	45	33.8	26.3	26.4	26.5	26.9
11.85	29.3	37.7	33.2	33.2	33.2	32.4
9.9	36.9	35.4	30.3	30.0	29.9	30.1
9.92	43.6	28.8	27.8	27.6	27.5	28.1
13.31	36.9	24.2	29.1	29.3	29.3	29.1
9.28	35	36.2	31.3	31.0	30.9	30.9
9.54	35.9	36.3	30.8	30.5	30.4	30.5
33.6	122.1	17.7	12.3	13.5	14.3	14.7
31.7	109.7	19.6	13.3	14.5	15.3	15.7

Fig. 4 and Table 1 show the deviation of Eq. (48) becomes much less than those of Eq. (38) and Eq. (43), showing the reliability of our theoretical model given in Eq. (47).

4. Discussion and Conclusions

If data for the porosity size is segmented, the following one can be considered:

$$F = K_r F_0 (1-\varphi)^{2/3} \sum_{i=1}^{N} a_i \left(\frac{r_{i0}}{r_{im}}\right)^{\alpha_i} , \quad \sum_{i=1}^{N} a_i = 1 \tag{49}$$

where r_{im} is the *i-th* segment's average radius, r_{i0} is the *i-th* segment's reference radius, which can be the segment's largest radius, a_i is the weighting factor.

If the pores are distributed continuously, then we have

$$F = KF_0(1-\varphi)^{2/3}\int_{r_{\min}}^{r_{\max}} \frac{(r_0)^n}{r^{n+1}}\,dr \tag{50}$$

This paper suggests some conformable formulations for estimating the strength of a porous concrete, making it applicable to various cases, and shedding new light on the optimal design of the porous concrete with a given strength. In our theory, particles' size distribution might be useful for practical applications.

Though our mathematical dimensionless model is mathematically correct and physically relevant, experimental verification is very much needed in future, and the fractal-fractional calculus [53,54] can be used for dynamical analysis of the porous concrete.

Acknowledgement: *The authors would like to acknowledge the National Key Research and Development Program of China (2019YFC1907105), National Natural Science Foundation of China (52178251), Xi'an Science and Technology Plan Key Project (2022JH-ZCZC-0026) for financial support.*

REFERENCES

1. Xue, R.J., Liu, F.J., 2022, *A fractional model and its application to heat prevention coating with cocoon-like hierarchy*, Thermal Science, 26(3), pp. 2493-2498.
2. Mo, X.X., Lu, Y.H., Liu, F.J., 2022, *Research on the design and performance of multilayer textiles with a cocoon-like hierarchy*, Journal of the Textile Institute, 113(12), pp. 2722-2731.
3. Xue, R.J., Mo, X.X., Liu, F.J., 2021, *Tussah cocoon's biomechanism: Fractal insight and experimental verification*, International Journal of Thermal Sciences, 169, 107089.
4. Wang, D.W., Li, F., Liu, M., Lu, G.Q., Cheng, H.M., 2008, *3D aperiodic hierarchical porous graphitic carbon material for high-rate electrochemical capacitive energy storage*, Angewandte Chemie-International Edition, 47(2), pp. 373-376.
5. Hou, J.H., Cao, C.B., Idrees, F., Ma, X.L., 2015, *Hierarchical Porous Nitrogen-Doped Carbon Nanosheets Derived from Silk for Ultrahigh-Capacity Battery Anodes and Supercapacitors*, ACS Nano, 9(3), pp. 2556-2564.
6. He, C.H., Amer, T.S., Tian, D., Abolila, A.F., Galal, A.A.,2022, *Controlling the kinematics of a spring-pendulum system using an energy harvesting device*, Journal of Low Frequency Noise Vibration and Active Control, 41(3), pp. 1234-1257.
7. Wang, Q.L., He, J.H., Liu, Z., 2022, *Intelligent Nanomaterials for Solar Energy Harvesting: From Polar Bear Hairs to Unsmooth Nanofiber Fabrication,* Frontiers in Bioengineering and Biotechnology, 10, 926253.
8. Yin, N., Liu, F.J., 2021, *Nanofibrous Filters for PM2.5 Filtration: Conception, Mechanism and Progress*, Nano, 16(4), 2130004.
9. Meng, D.P., Zhang, Y.H., Wu, J.T., 2022, *Graphene/polyimide nanofibrous mat for high-efficiency filtration,* AATCC Journal of Research, 9 (4), pp. 176-181.
10. Robert, B., Nallathambi, G., 2022, *Tailoring mechanically robust nanofibrous membrane for PM2.5-0.3 filtration and evaluating their behaviour using response surface Box-Behnken design*, Separation Science and Technology, 57 (16), pp. 2583-2595.
11. Cheng, X., Zhao, L., Zhang, Z.W., et al., 2022, *Highly efficient, low-resistant, well-ordered PAN nanofiber membranes for air filtration*, Colloids and Surfaces A: Physicochemical and Engineering Aspects, 655, 130302.
12. He, J.H., Qian, M.Y., 2022, *A fractal approach to the diffusion process of red ink in a saline water*, Thermal Science, 26(3B), pp. 2447-2451.
13. Gao, J., Xiao, B.Q., Tu, B.L., et al., 2022, *A fractal model for gas diffusion in dry and wet fibrous media with tortuous converging-diverging capillary bundle*, Fractals, 30(9), 2250176.
14. Li, Z.Y., Chen, Q.T., Wang, Y.L., Li, X.Y., 2022, *Solving two-sided fractional super-diffusive partial differential equations with variable coefficients in a class of new reproducing kernel spaces*, Fractal and Fractional, 6(9), 492.

15. Wang, K.J., 2022, *Variational principle and approximate solution for the fractal vibration equation in a microgravity space*, Iranian Journal of Science and Technology-Transactions of Mechanical Engineering, 46(1), pp. 161–165.
16. Feng, G.Q., 2021, *He's frequency formula to fractal undamped Duffing equation*, Journal of Low Frequency Noise Vibration and Active Control, 40 (4), pp. 1671-1676.
17. Feng, G.Q., Niu, J.Y., 2021, *He's frequency formulation for nonlinear vibration of a porous foundation with fractal derivative*, GEM-International Journal on Geomathematics, 12(1), 14.
18. Babič, M., Fragassa, C., Lesiuk, G., Marinković, D., 2020, *A new method for complexity determination by using fractals and its applications in material surface characteristics*, International Journal for Quality Research, 14(3), pp. 705-716.
19. Babič, M., Marinkovic, D., Bonfanti, M., Calì M., 2022, *Complexity Modeling of Steel-Laser-Hardened Surface Microstructures*, Applied Sciences, 12(5), 2458.
20. Babic M., Lesiuk G., Marinkovic D., Calì M., 2021, *Evaluation of microstructural complex geometry of robot laser hardened materials through a genetic programming model*, Procedia Manufacturing, 55(C), pp. 253-259.
21. Varzaneh, A.S., Naderi, M., 2022, *Experimental and Finite Element Study to Determine the Mechanical Properties and Bond Between Repair Mortars and Concrete Substrates*, Journal of Applied Computational Mechanics, 8 (2), pp. 493-509.
22. Mander; J. B., Priestley, M. J. N., Park, R., 1988, *Theoretical Stress-Strain Model for Confined Concrete*, Journal of Structural Engineering-ASCE, 114 (8), pp. 1804-1826.
23. Lee, J.H., Fenves, G.L., 1998, *Plastic-damage model for cyclic loading of concrete structures*, Journal of Engineering Mechanics-ASCE, 124 (8), pp. 892-900.
24. Mandelbrot, B. B., 1967, *How long is the coast of Britain? Statistical self-similarity and fractional dimension*, Science, 156(3775), pp. 636–638.
25. Zuo, Y.-T., Liu, H.-J., 2021, *Fractal approach to mechanical and electrical properties of graphene/sic composites*, Facta Universitatis-Series Mechanical Engineering, 19(2), pp. 271-284.
26. Mandelbrot, B.B., Passojat, D.E., Paullay, A.J., 1984, *Fractal character of fracture surfaces of metals*, Nature, 308 (5961) , pp. 721-722.
27. Feng, Y.J., Yu, B.M., Zou, M.Q., Zhang, D.M., 2004, *A generalized model for the effective thermal conductivity of porous media based on self-similarity*, Journal of Physics D, 37(21), pp. 3030-3040.
28. Kong, H.Y., 2015, *Research on Principle of Bubble Electrospinning and Morphologies Controlling and Applications of Bubble Electrospun Nanofibers*, PhD Thesis, Soochow University; DOI: 10.7666/d.D658152
29. Gao, J., Pan, N., Yu, W.D., 2007, *Golden mean and fractal dimension of goose down*, International Journal of Nonlinear Sciences and Numerical Simulation, 8 (1), pp. 113-116.
30. Fan, J., Yang, X., Liu, Y., 2019, *Fractal calculus for analysis of wool fiber: Mathematical insight of its biomechanism*, Journal of Engineered Fibers and Fabrics, 14, doi: 10.1177/1558925019872200
31. Rieu, M., Sposito, G., 1991, *Fractal Fragmentation, Soil Porosity, and Soil Water Properties: I. Theory*, Soil Science Society of America Journal, 55(5), pp. 1231-1238.
32. Yu, B.M., 2007, *Comments on "Fractal Fragmentation, Soil Porosity, and Soil Water Properties: I. Theory"*, Soil Science Society of America Journal, 71 (2), pp. 632-632.
33. He, J.H., 2021, *Seeing with a single scale is always unbelieving: From magic to two-scale fractal*, Thermal Science, 25 (2), pp. 1217-1219.
34. Nadeem, M., He, J.-H.,2022, *The homotopy perturbation method for fractional differential equations: part 2, two-scale transform*, International Journal of Numerical Methods for Heat & Fluid Flow, 32(2), pp. 559-567.
35. Ain, Q. T., Sathiyaraj, T., Karim, S., et al., 2022, *ABC Fractional Derivative for the Alcohol Drinking Model using Two-Scale Fractal Dimension*, Complexity, 2022, 8531858.
36. Elias-Zuniga, A ., 2022, *On the two-scale dimension and its application for deriving a new analytical solution for the fractal Duffing's equation,* Fractals, 30(3), 2250061.
37. Elias-Zuniga, A., Palacios-Pineda, L.M., Olvera-Trejo, D., Martinez-Romero, O., 2022, *Recent strategy to study fractal-order viscoelastic polymer materials using an ancient Chinese algorithm and He's formulation*, Journal of Low Frequency Noise Vibration and Active Control, 41(3), pp. 842-851 .
38. He, J.H., El-Dib, Y.O.,2021, *A tutorial introduction to the two-scale fractal calculus and its application to the fractal Zhiber-Shabat Oscillator*, Fractals, 29(08), 2150268.
39. Yang, J.R., Afzal, F., Appiah, P., 2022, *Fractional Derivative for Varicella-Zoster Virus Using Two-Scale Fractal Dimension Approach with Vaccination*, Advances in Mathematical Physics, 2022, 1725110
40. Yao, S.W., 2021, *A rigid pendulum in a microgravity: some special properties and a two-scale fractal model*, Fractals, 29(6), 2150127 .
41. Balshin, M.Y., 1949, *Relation of mechanical properties of powder metals and their porosity and the ultimate properties of porous metal-ceramic materials*, Dokl. Acad. Nauk SSSR, 67, pp. 831- 834.

42. Tang, L. P., 1986, *A study of the quantitative relationship between strength and pore-size distribution of porous materials*, Cement and Concrete Research, 16, pp. 87-96.
43. Kumar, R., Bhattacharjee, B., 2003, *Porosity, pore size distribution and in situ strength of concrete*, Cement and Concrete Research, 33, pp. 155–164.
44. Estrada-Diaz, J.A., Olvera-Trejo, D., Elias-Zuniga, A., Martinez-Romero, O., 2021, *A mathematical dimensionless model for electrohydrodynamics*, Results in Physics, 25, 104256.
45. He, C.H., Liu, S.H., Liu, C., Mohammad-Sedighi, H., 2022, *A novel bond stress-slip model for 3-D printed concretes*, Discrete and Continuous dynamical Systems, 15(7) , pp. 1669-1683.
46. He, J.H., Wan, Y.Q., Xu, L., 2007, *Nano-effects, quantum-like properties in electrospun nanofibers,* Chaos Solitons & Fractals, 33(1), pp. 26-37 .
47. Tian, D., Li, X.X., He, J.H., 2019, *Geometrical potential and nanofiber's highly selective adsorption property,* Adsorption Science & Technology, 37 (5-6), pp. 367-388.
48. Wu, P.X., Ling, W.W., Li, X.M., He, X.C., Xie, L.J., 2022, *Dynamics research of Fangzhu's nanoscale surface,* Journal of Low Frequency Noise Vibration and Active Control, 41 (2), pp. 479-487.
49. Elías-Zúñiga, A., Palacios-Pineda, L.M., Jiménez-Cedeño, I.H., Martínez-Romero, O., Trejo, D.O.,2020, *He's frequency–amplitude formulation for nonlinear oscillators using Jacobi elliptic functions*, Journal of Low Frequency Noise, Vibration and Active Control. 39(4), pp. 1216-1223.
50. Fan, J., Zhang, Y.R., Liu, Y., et al., 2019, *Explanation of the cell orientation in a nanofiber membrane by the geometric potential theory*, Results in Physics, 15, 102537 .
51. Tian, D., Zhou, C.J., He, J.H., 2018, *Hall-Petch effect and inverse Hall-Petch effect: A fractal unification*, Fractals, 6(26), 1850083.
52. West, G.B., Brown, J.H., Enquist, B.J., 1999, *The fourth dimension of life: Fractal geometry and allometric scaling of organisms*, Science, 284 (5420), pp. 1677-1679.
53. Atangana, A., 2017, *Fractal-fractional differentiation and integration: Connecting fractal calculus and fractional calculus to predict complex system*, Chaos, Solitons & Fractals, 102, pp. 396-406.
54. Li, Z.Y., Wang, M.C., Wang, Y.L., 2022, *Solving a class of variable order nonlinear fractional integral differential equations by using reproducing kernel function*, AIMS Mathematics, 7(7), pp. 12935-12951.